

# RADAR-DERIVED DEMS FOR URBAN AREAS

**J. Bryan Mercer  
Michael Gill**

**Intermap Technologies Ltd.  
900, 645 - 7th Ave. S.W.  
Calgary, Alberta  
Canada T2P 4G8**

**tel: (403) 266-0900  
fax: (403) 265-0499  
e-mail: bmercerc@intermap.ca**

## ABSTRACT

The role for Digital Elevation Models (DEMs) has been expanding rapidly in recent years. Applications are increasing and encompass industries as diverse as telecommunications, forestry, municipal engineering and precision agriculture to name only a few. The accuracy and detail required varies with application, and a number of technologies are able to provide DEMs appropriate to particular mapping scales. To date, DEM availability, accuracy and price issues have tended to be a disincentive for many users. The problem is evident on a global basis. However, even in the well mapped areas of North America and Europe there is a desire from users for more detail over broader areas and at lower cost.

In response to this perceived demand, Intermap Technologies has commenced the development of a data bank of medium and high detail/accuracy DEMs under the name of Global Terrain™. In particular, it is the goal to create a DEM data base of 5 meter postings and 1.5 meter ( $1\sigma$ ) vertical accuracy for large portions of North America and Europe over the next two years. Most of this data base will be created using STAR-3i, an interferometric airborne SAR carried in a Lear Jet. STAR-3i has been operated commercially by Intermap since January 1997. Its products include DEMs and Ortho-Rectified Images (ORIs), both acquired at sample spacing of 2.5 meters although normally averaged down to 5 meters or coarser.

Previous application areas for radar have typically been rural. Because of the spatial detail now available with STAR-3i, and with the price competitiveness afforded by the Global Terrain™ strategy, there is now considerable interest in the applicability of these DEMs and ORIs for urban applications such as mobile telecommunications. However, urban areas are very complex as seen by the radar, and there are a number of effects that may impact the appearance of the DEM and/or the ORI. This work reports on the 'performance' of STAR-3i

DEMs in two urban test areas of Denver, Colorado, USA. The test areas were chosen to be representative of industrial, high-rise and low-rise residential regions outside the dense urban core. As a basis of comparison, DEMs and ortho-rectified images from air-photos were acquired from a commercial vendor for both areas. Additionally, a high precision DEM derived from an airborne laser scanning system was obtained for one of the areas. This paper reports on the results to-date of the comparison. In order to put the results in context, the various factors that contribute to the observed DEM response to buildings and other objects are examined.

A major objective of the work, which is on-going, is to determine to what extent the STAR-3i DEM can be used for 3D building extraction and, on the other hand, for creation of a 'bald-earth' DTM. In this paper we provide illustrations and statistical data to demonstrate the viability of STAR-3i DEMs for both of these applications in a typical North American city. The Global Terrain™ DEMs therefore represent a technically attractive and cost competitive alternative for many urban applications.

## 1. Introduction

Digital Elevation Models (DEMs) are being used increasingly at a variety of mapping scales, and for a range of applications. The DEM price, irrespective of technology, tends to vary with the level of detail sought – that is, with the desired mapping scale (Mercer, et al., 1997). The introduction of DEMs created from radar in recent years has expanded the circumstances under which DEMs can be collected owing to the capability to collect data in day/night, cloud-covered conditions. This factor positively impacts both the timeliness and the price of DEMs. Interferometric radar (IFSAR) has received much attention recently because of its potential to improve the level of detail achievable in radar-derived DEMs. In the past year, about a quarter million kmsq of

DEM have been acquired over several continents by the new STAR-3i system, an airborne interferometric SAR (Synthetic Aperture Radar), owned and commercially operated by Intermap Technologies. With data collected and presented at sample spacings down to 2.5 meters and with better than 2 meter (RMS) vertical and horizontal accuracies, this presents users with the possibility of obtaining wide area DEM coverage at levels of detail and consistency not previously available in general.

The STAR-3i system is an X-band radar and the DEM derived from it references the scattering surface or volume with which the radar beam interacts. This means that scattering objects such as trees or buildings will contribute to the radar-derived DEM. This problem is similar to that of photo-derived DEMs but of course the radar has its own particularities. In this paper we present preliminary results of some comparative tests done in urban situations where the presence of buildings of different types and of typical tree growth are reflected in the radar-derived DEM. The objective was to determine, in these urban examples, what elevation information can be extracted: in particular, to what extent DEMs created from STAR-3i correctly represent building structures, and to what extent a bald-earth DEM could be extracted from these DEMs. In the following paragraphs, the term DEM refers to the implied elevation of whatever the scattering surface happens to be. We refer to the underlying bald-earth elevation model as a DTM (Digital Terrain Model). In both cases they consist of a raster grid of elevation values with reference to the WGS84 ellipsoid. Over small test areas the geoid undulation is sufficiently small to ignore.

## 2. Interferometry Background

The interferometric process has been widely discussed in the literature, particularly for the case of repeat pass interferometry (e.g. Zebkor and Villsenor (1992), Goldstein et al., (1988)). Some of the general issues associated with airborne interferometry have been discussed, for example, in Gray and Farris-Manning (1993) and Madsen et al. (1991). The geometry relevant to height extraction, 'h', is illustrated in Figure 1.

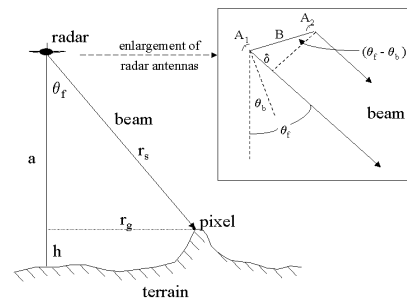


**Figure 1. Schematic of Airborne IFSARE Geometry.**

If the two antennas, separated by baseline 'B', receive the back-scattered signal from the same ground pixel, there will be a path-difference ' $\delta$ ' between the two wavefronts. The baseline angle ' $\theta_b$ ' is obtainable from the aircraft inertial system, the aircraft height is known from DGPS and the distance from antenna to pixel is the radar slant range. Then it is simple trigonometry to compute the target height 'h' in terms of these quantities. The path-difference is measured indirectly from the phase difference between the received wavefronts. Because the phase difference can only be measured between 0 and  $2\pi$  (modulo  $2\pi$ ), there is an absolute phase ambiguity which is normally resolved with the aid of ground control and a "phase unwrapping" technique (e.g. Goldstein et al, 1988). Thus the extraction of elevation is performed on the "unwrapped" phase.

## 3. System Specifications and Performance

Intermap Technologies, through agreements with ERIM and DARPA (Defense Advanced Projects Agency), have obtained exclusive rights to market and operate the IFSARE airborne SAR system developed by ERIM. The system has been re-named STAR-3i. The IFSARE system was described by Sos, et. al. (1994), and is briefly summarized from an operational point of view in the following paragraphs. The first commercial operations of STAR-3i commenced in December, 1996.

STAR-3i, an X-band, interferometric SAR, is carried in a LearJet 36 and is capable, under ideal circumstances, of imaging 30,000 km<sup>2</sup> in a single operational day. Positioning and motion compensation are achieved through use of a coupled laser inertial reference platform and GPS which is differentially post-processed. One of its operational mission modes would be performed at 40,000' (12.2 km) ASL and in this mode it would collect 2.5 meter pixels across a 10 km ground swath. At lower altitudes, the signal-to-noise ratio is larger and thus the height noise is lower (Zebker and Villasenor, 1992) thereby improving relative accuracy; however,

swath width is reduced. The DEM created from the interferometric data is post-processed, and an ortho-rectified image (ORI) is simultaneously produced.

Processing is currently performed on a local network of Ultra SPARC II workstations with rather large amounts of disk and memory. Work currently underway will result in a new processor which will enable field processing and quasi-real time throughput performance.

The main system parameters have been described elsewhere (Mercer et al, (1997), and Sos, et al, (1994)).

Independent tests (Carling, 1996 and Norvelle, 1996) as well as internal tests have been performed to evaluate accuracy in the vertical and horizontal. Under 'bald earth' conditions – that is, in test areas devoid of vegetation - and in the high altitude (40,000 ft) flight mode, vertical performance for DEMs with 5 meter sample spacing was at the 1.5 meter level ( $1\sigma$ ) with respect to typical offsets of about 1.5 m absolute. Recent tests in Germany at lower altitude (20,000 ft), conducted by the Institute of Navigation at Stuttgart, University have shown 0.7-1.0 m ( $1\sigma$ ) height accuracy (relative to a 1.3 m mean offset) over sub-regions of several km.

#### 4. Urban Performance

In this paper, we are exploring the STAR-3i performance under urban conditions in which structures of various footprints, heights and densities impact the observed DEMs. Additionally there are trees, vehicles, lamp-posts and other objects that contribute to the response of the system. The intention in this study is to examine the performance of the radar system in comparison with 'truth' to the extent that 'truth' is available. Although it is not intended to provide a theoretical analysis in this work, there are a number of radar and algorithmic issues that we might expect to have an impact on the observations, and these are summarized below as a framework within which to assess the results.

##### 4.1 Radar Issues in Urban Areas

Some of the expected issues, associated with radar/building interaction, are listed below with brief descriptions. Certain of these are generic with respect to radar, while others relate to the particular system (STAR-3i) and the processing algorithms implemented. In the following consider the situation of Figure 2 in which a hypothetical flat-topped building is an isolated target object.

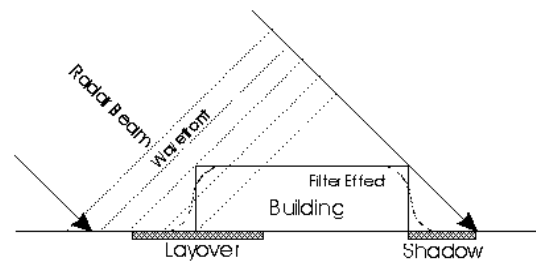


Figure 2. Radar/Building Interaction Schematic.

- Shadows are created at the trailing edge of the building. Simple geometry applies and it would be expected in this instance ( $\sim 45^\circ$  incidence at mid-swath) that the shadow length would approximate the building height. All information is lost in shadow regions. However, filtering of the interferogram or phase image, may partially mitigate this effect.
- The shadow interface with the building in its un-rectified form would be displaced toward the radar. Upon ortho-rectification, and using the elevation created from the same data set, it would, in principle be returned to its correct location. Departures from this would depend on the accuracy of the derived elevation, possible re-sampling effects, filtering effects and phase unwrapping issues.
- Layover would probably cause elevation information to be lost, depending on the relative magnitudes of the scattering cross-sections of the fore-ground, near-side and top near-side of the building. For the STAR-3i incidence angle ( $\sim 45^\circ$  at mid-swath), the total horizontal region of uncertainty is approximately equal to twice the height of the building.
- For noise-reduction purposes, an operator-selectable filter is normally implemented, which smooths the phase and has the effect of averaging over step function height discontinuities in a quasi-linear fashion.
- The specific implementation of the phase unwrapping algorithm in response to step-function phase changes will impact the derived elevation.
- Multipath effects can cause ghosting although this has not been specifically identified in the data sets used in this study.

If tall buildings are clustered closely together as in core city areas, it would be expected that the combined effects of the foregoing would contribute to a confusing set of observations. For this reason, we have confined this set of tests to two areas outside the city core where most of these effects might be observed in relatively unambiguous fashion.

##### 4.2 Test Description

#### 4.2.1 The Test Areas

Several swaths of STAR-3i data were acquired by Intermap, of parts of the Denver, Colorado urban area on August 25, 1997. Two areas, each about 2.5 km<sup>2</sup> (1 sq mile) were extracted for study. The test areas are referred to as Leetsdale and Santa Fe, respectively, after local street names. The radar flight path was 10° off a north/south line (radar viewing angle from the east (~80°)) which helped simplify subsequent analysis.

Leetsdale is a mixed urban area with several large, relatively isolated apartment tower buildings (heights ranging from 10 to 40 meters above the surrounding ground level), urban streets with typical 1-2 story houses and surrounding yards and trees, plus a few open park areas. Santa Fe is an industrial area with a number of wide warehouse structures along with some open areas.

#### 4.2.2 The Data Sets

The STAR-3i data included DEMs, with associated ORIs and Correlation Images, on a 2.5 meter UTM grid referenced to WGS-84. When shadows, low signal-to-noise or layover effects cause correlation between the two antennas to drop below a pre-selected value for a particular pixel, that pixel value was flagged as 'no data'. DEMs were manipulated in 16 bit form restricting precision to about 0.3 meters which was adequate for these purposes.

Aerial photo data were acquired commercially from Image Scans Inc of Denver, Colo. for these same two areas. These data included ORIs from their City Scenes™ product line as well as the underlying DEMs. The ORIs were subsequently resampled by Intermap from 0.5 meter pixels to 2.5 meter pixels on the same grid as the radar data. Similarly, the photo-derived DEM data were re-sampled from 2 meters to 2.5 meters. The photo-DEM, derived from archived USGS stereo photos with standard 60 % overlap, were expected to have vertical uncertainty about 2 meters (1σ) (Rob Ledner, Private Communication), similar to the radar DEM. It was expected (ibid) that the reliability of the photo DEM would deteriorate for building heights above ~10-15 meters owing to the stereo geometry. It should also be noted that the archived photos were up to five years older than the radar data, so there would be some changes in the scene areas expected.

Recently, it was possible to acquire commercially available laser data for one of the areas (Leetsdale) from EagleScan Corp. of Boulder, Colorado. These elevation data were also re-sampled to the common 2.5 meter grid from a point collection with specified sampling density of 3-5 meters and 15 cm (1σ) vertical uncertainty.

Radar, photo and laser data were ingested into a commercial software package (Vertical Mapper™, a product of Northwood Geosciences, Ottawa, Ontario). It was necessary to normalize the different data sets by a few meters in the vertical for reasons not understood but associated perhaps with datum issues. The shift was about 7 meters in one case (photo-to-radar) and 3 meters in the other (laser-to-radar). This was not an issue for purposes of this study. It was also possible to check for horizontal consistency among the sets using ORIs where possible and street patterns visible in the DEMs. It was necessary to translate the photo data because of the datum difference, while the laser data were in the same horizontal system as the radar, and global offsets were observed to be sub-pixel.

Because the data sets were in common raster-based form it was possible to intercompare them easily using Vertical Mapper's functionality. Several analytical procedures were performed:

- Elevation profiles were run across buildings or groups of buildings as identified in the aerial photos. Profiles were run E-W and N-S (essentially parallel and perpendicular, respectively, to the radar beam direction).
- Colorised elevation plots were created for the DEMs from all data sets.
- Elevation 'Difference Surfaces' (STAR-3i – Photo) or (STAR-3i – Laser) were created and plotted as colorised maps, where the quantity in brackets references the DEM elevation differences on a pixel-to-pixel basis (more correctly sample-to-sample basis, each sample being at 2.5 meters spacing).
- Mean difference and RMS statistics of these difference surfaces or of sub-sets were calculated.
- Building 'DEM footprints' were manually vectorised as rectangles for intercomparison.
- A simple bald-earth model was extracted using two complementary methods (interpolation from points thought to represent ground level, and, removal of objects thought to be buildings, followed by interpolation).
- Simple building models were generated, based upon the maximum height and the manually extracted DEM footprint.

### 4.3 Results

#### 4.3.1 Santa Fe Test Sub-Set

A sub-set of the area tested is shown in Figures 3 through 6. The STAR-3i image shows the sub-area with several of the warehouse-type buildings outlined. Typical building dimensions are about 100 meters on a side. In Figure 4 we show a colorised DEM of one of the buildings and its surroundings.

The trace drawn upon the building corresponds to an elevation profile displayed in Figure 5. Several effects can be seen:

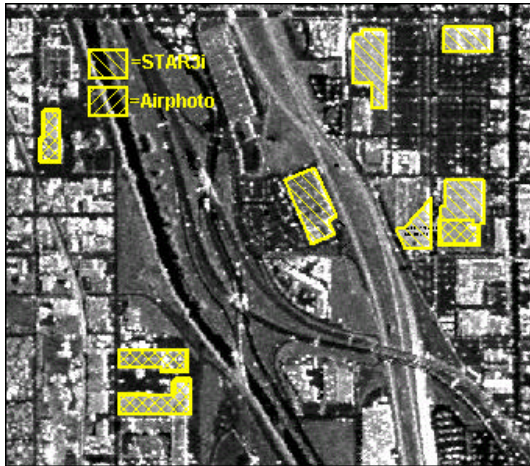


**Figure 3. STAR-3i Ortho-Rectified Image of Santa Fe area. The hatched rectangle in the middle, right-hand side is the building shown in Figures 4-6.**

- The mean height above the surrounding ground level is about 10 meters and the roof is quite flat. Elevation 'noise' is apparently less than 30 cm, although other profiles across the same roof have shown there to be objects on the roof apparently about 75cm high. A selection of seven similar buildings in the area were sampled for rooftop variability which would include true 'noise' plus real variability due to objects such as ventilators, refrigeration units, etc. The standard deviation about the rooftop mean height in each case was tabulated, with results that varied from 23 cm to 83 cm.

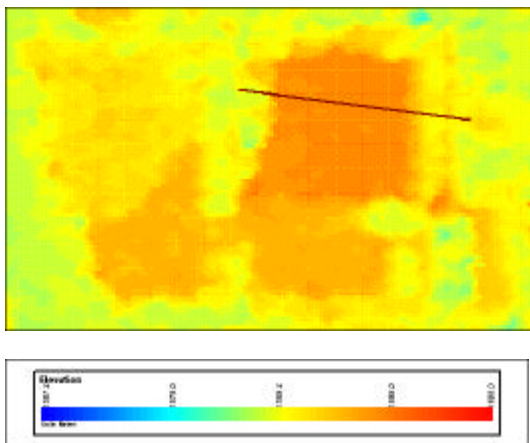


**Figure 4. STAR-3i DEM of 500 meter sub-area. Elevations vary from 1,580 to 1,600 meters. Note profile location.**

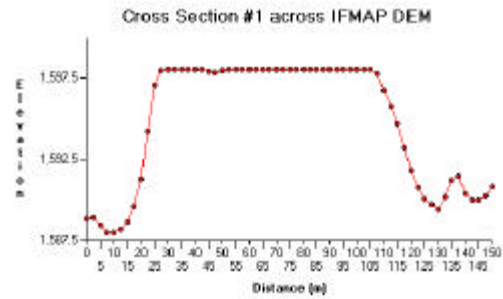


**Figure 5. Profile across warehouse building shown in Figure 4.**

- The sides of the building show the filter response. A similar response is observed for profiles in the orthogonal direction. Assuming that the building walls are vertical, the filter appears to broaden the footprint by about 3 - 4 pixels, corresponding to 7.5 - 10 meters, on each side.
- Comparison of building footprints with the photo-derived DEM shows outlines which in most cases are within a few meters of one another. The photo-DEM and the radar-DEM are both ortho-rectified and in the absence of error, filtering, and sampling issues, would be expected to be identical.
- Comparison of the difference surface (STAR-3i - Photo) of the DEMs is shown in figure 6. The large discrepancy, coloured as solid red, exemplifies a building which was constructed

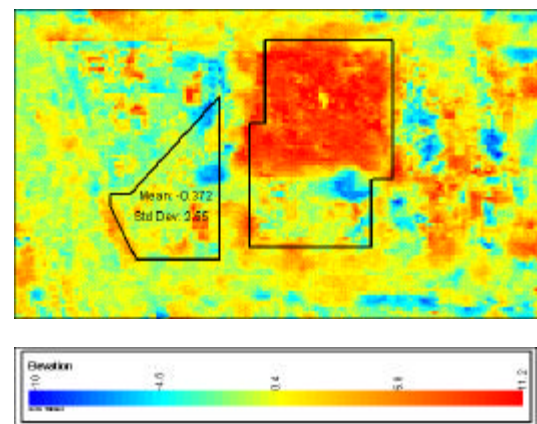


**Figure 6. Elevation difference surface (STAR-3i photo DEM) of same area (see text).**

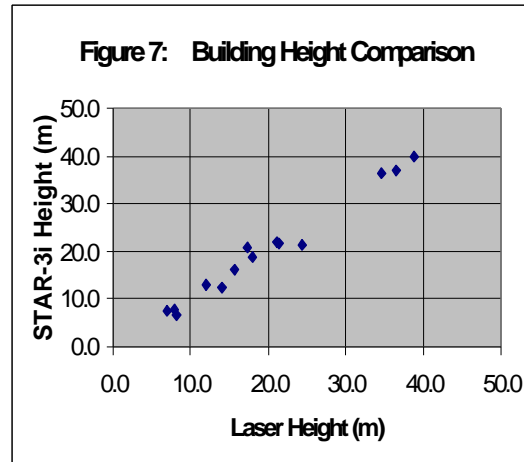
- after the air-photos were obtained, but captured in the radar DEM. The degree to which the two DEMs compare overall is provided by the difference statistics. In the sub-area denoted by the rectangle, the standard deviation of the elevation difference is 2.6 meters. Compared to the radar elevation noise level noted above, it suggests that much of the difference is due to noise in the photo-DEM plus building edge effects and probably other objects (vehicles, etc.) that were in one DEM but not the other.
- It is interesting to note that no data dropouts are observed in the radar DEM in this set due to expected 5-10 meter shadow or layover effects. This is believed due to the filter bridging these small gaps.
- A bald earth DEM was created for this area by two methods as noted earlier. Space limitations preclude display, but in general it appears that the ground point sub-sampling provides a smoother DEM albeit with some artifacts associated with the ground sampling patterns. Comparison of the two approaches reveals very small mean differences (~0.5 m) of the derived bald-earth DTMs over sub-areas of about 0.5 km, and smaller scale differences of about 2 m ( $1 \sigma$ ).

#### 4.3.2 Leetsdale Test Sub-Set

The main objective in the case of the Leetsdale area was to determine to what extent the STAR-3i DEM could reproduce the heights of the local high-rise apartment structures. Secondly it was expected that data dropouts caused by shadow and layover effects would be observed as noted earlier. Moreover, because the building heights were often greater than their width (in the radar range direction), it was anticipated that some anomalous behavior might be observed. However it was hoped that it would be possible to extract the building footprint either from the radar DEM or ORI in order to permit the three dimensional approximations of these buildings as parallelepipeds.

Because the air-photo DEMs were of use only for the lower buildings, the laser DEM was used as truth for much of this analysis. A set of 10 buildings were selected, ranging in height from 7 to 40 meters. Maximum elevations were extracted for each building in both the radar and laser DEMs. Similarly the ground levels were determined as the average elevations near the footprint that could be unambiguously identified as bald earth. The heights were defined as the elevation difference of these

quantities and the results are shown as a regression plot in Figure 7.



The correlation is very strong. Upon comparison of the height differences (STAR-3i – Laser), the mean difference is 0.3 meters and the standard deviation is 1.5 meters. It should be noted that the roofs of these buildings were relatively flat although they appeared to have elevator housings on at least some of them.

A similar regression of apparent building widths derived from the DEMs showed the radar footprints to be about 10 meters wider on average than the laser footprints. This presumably is due to the filter effect in the radar.

The largest buildings showed dropouts fore and aft in the radar DEM, consistent with the layover and shadow expectations noted earlier.

An unexpected observation was that the taller buildings exhibited a shift of the DEM footprint towards the radar. The centroid of the footprint was measured and the offset from truth calculated and plotted as a function of height. Most of the offsets were correlated with building height reaching a maximum offset of about 12 meters. Reasons for this anomaly are under investigation, but it is currently believed that this is a correctable algorithmic problem.

In Figure 8 we present a perspective view of the reconstructed buildings that were extracted from the STAR-3i DEM using footprints and maximum building heights. These are the buildings used in the height regression analysis of Figure 7.



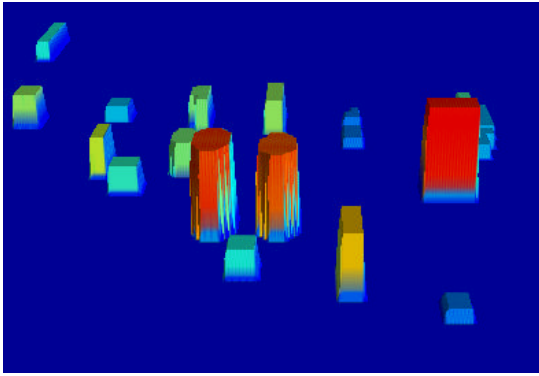


**Figure 8. Perspective view of buildings modelled from STAR-3i DEM.**

## 5. Conclusions

In this paper we have compared STAR-3i DEMs against those derived from stereo air-photo (archived 60% overlap source data) and airborne laser scanner. The test areas included two urban-type areas, typical of North American cities, containing a variety of buildings and other objects. Comparative examples were shown and statistical comparisons made. The results generally were consistent with a number of factors that were described in the context of expected radar/building interaction. It was determined that:

- When compared to the air-photo DEMs in the areas of low warehouse type buildings, the radar DEMs were of somewhat superior quality. In fact upon examining the radar height noise on large flat roofs, 0.5 m ( $1 \sigma$ ) performance level was observed. In general, the elevation difference between the two DEMs was characterized statistically by about 2.5 meters ( $1 \sigma$ ) which includes the relative 'noise' contributions from both, as well as apparently real differences due to target changes between acquisition dates.
- In the Leetsdale test area where isolated high-rise apartment buildings were the targets of interest, the radar DEMs were compared with airborne laser DEMs as 'truth'. The radar-derived building heights corresponded closely to those of the laser system with scatter of about 1.5 meters over a height range of 6 – 40 meters.
- Among the larger buildings, typically above 20 meters height, effects of radar shadow and layover created data dropouts as expected. Filtering effects also made the building footprints somewhat wider than reality (~10-15 meters).
- It was possible to model individual buildings, in a simple, three dimensional sense from the radar DEM data (specifically from the DEM-derived height and footprint). This statement refers to

warehouse type buildings and to apartment or office type buildings provided they are relatively isolated.

It appears, therefore, that in urban areas (excluding the dense built-up core areas) the STAR-3i DEM can be used very effectively for many applications. The radar alternative is considerably less expensive than the alternatives at a similar level of detail, and should therefore allow wider use of DEMs for telecommunications and other markets.

## 6. Acknowledgments

The DEMs created from air-photo and from airborne scanning laser were obtained commercially under license from Image Scans Inc. of Boulder, Colo. and from Eaglescan Corp. respectively. We wish to thank Rob Ledner of Vexcel Corp. for technical insight into the air-photo DEMs. We would also like to thank our Intermap colleagues in the airborne radar group for providing the radar data and for helpful discussions..

## 7. References

- Carling, Robert, (1996). GeoSAR Program; IFSAR Validation and Terrain Classification from Polarimetry. Presentation to SPIE Conference, Orlando, FL.
- Gray, Laurence A., and P.J. Farris-Manning, (1993). Repeat-Pass Interferometry with Airborne Synthetic Aperture Radar. IEEE Transactions on Geoscience and Remote Sensing. Vol. 31: Number 1, pp 180-191.
- Goldstein, R.M., H.A. Zebker, and C. Werner, (1988). Satellite Radar Interferometry: two dimensional phase unwrapping. Radio Sci. Vol. 23: Number 4, pp 713-720.
- Madsen, Soren N., H.A. Zebker, and Jan Martin, (1991). Topographic Mapping Using Radar Interferometry: Processing Techniques. Pre-print submitted to IEEE Geoscience and Remote Sensing December 6, 1991.
- Mercer, J.B., S. Thornton, and K.Tennant, (1997). Creation of DEMs from RADARSAT Stereo and from Airborne Interferometry. Proceedings of the Joint ISPRS Workshop, 'Sensors from Space'.
- Norvelle, F. Raye, (1996). Evaluation of ERIM's IFSARE Digital Elevation Models of Cholame Hills and Camp Roberts, CA. Document Prepared for DARPA Sensor Technology Office.
- Sos, G. Tim, Herbert W. Klimach and Gray F. Adams, (1994). High Performance Interferometric

SAR Description and Capabilities. Tenth ERIM Thematic Conference on Geologic Remote Sensing, San Antonio, Texas, Vol. II, pp. 637-649.

Zebker, Howard A., and J. Villasenor (1992). Decorrelation in Interferometric Radar Echoes. IEEE Transactions on Geoscience and Remote Sensing, Vol. 30: Number 5, pp 950-959.